Agriculture, population growth, and statistical analysis of the radiocarbon record

H. Jabran Zahid[a,1], Erick Robinson[b,1], and Robert L. Kelly[b]

[a]Smithsonian Astrophysical Observatory, Harvard–Smithsonian Center for Astrophysics, Cambridge, MA 02138; and [b]Department of Anthropology, University of Wyoming, Laramie, WY 82071

Edited by Stephen J. Shennan, University College London, London, United Kingdom, and accepted by the Editorial Board November 10, 2015 (received for review September 4, 2015)

The human population has grown significantly since the onset of the Holocene about 12,000 y ago. Despite decades of research, the factors determining prehistoric population growth remain uncertain. Here, we examine measurements of the rate of growth of the prehistoric human population based on statistical analysis of the radiocarbon record. We find that, during most of the Holocene, human populations worldwide grew at a long-term annual rate of 0.04%. Statistical analysis of the radiocarbon record shows that transitioning farming societies experienced the same rate of growth as contemporaneous foraging societies. The same rate of growth measured for populations dwelling in a range of environments and practicing a variety of subsistence strategies suggests that the global climate and/or endogenous biological factors, not adaptability to local environment or subsistence practices, regulated the long-term growth of the human population during most of the Holocene. Our results demonstrate that statistical analyses of large ensembles of radiocarbon dates are robust and valuable for quantitatively investigating the demography of prehistoric human populations worldwide.

archeology | paleodemography | radiocarbon dating | hunter-gatherers | agriculture

The population is currently growing at an average rate of 1% per year with some countries exhibiting growth rates as large as a few percent or more (1). Such high growth rates are a phenomenon associated with modern industrial human societies and far exceed the average growth rates of prehistoric populations (2). The current rapid growth of the human species belies a humble beginning. Fossil evidence suggests that anatomically modern humans evolved some 200,000 y ago (3). Based on genetic studies of mitochondrial DNA, it appears that, for the first 100,000 y, humans inhabited Africa in relatively small, isolated groups existing on the brink of extinction (4). Perhaps driven by unstable environmental conditions, humans migrated 60,000–80,000 y ago (5) into Europe, Asia, and Australia (6, 7). At the dawn of the Holocene 12,000 y ago, humans had already arrived to the Americas (8), successfully populating virtually the whole planet.

The onset of the Holocene marked the transition to an epoch of significantly warmer temperatures, higher CO_2 content, and a relatively stable climate (9, 10). These environmental conditions are conducive to agriculture (11), which may have increased food productivity, thus accelerating population growth. Accelerated population growth associated with agriculture is sometimes referred to as the Agricultural or Neolithic Demographic Transition (12). The causal link between agriculture and accelerated population growth remains controversial (13–15).

Studies of prehistoric skeletal remains and genetic coalescent analysis are some of the most rigorous attempts to investigate a potential causal link between agriculture and accelerated population growth. Cemetery data show that fertility increased during the transition to agriculture (12, 16–18). However, mortality cannot be measured from these data, and thus the population growth rate is unknown (18). Accelerated growth also may be inferred from genetic diversity among modern populations. However, the conversion of genetic diversity into a growth rate is subject to several systematic uncertainties and thus far has yielded contradictory results regarding the impact of the agricultural transition on population growth (19–24).

Radiocarbon dates provide a direct record of prehistoric human activity, and large samples have been used for quantitative demographic analysis (25–30). Larger populations produce more datable material; thus, the temporal frequency of the radiocarbon record reflects the size of the population. Here, we use the summed probability distribution (SPD) of an ensemble of calibrated radiocarbon measurements, corrected for taphonomic loss (31), as a proxy for the relative size of a population as a function of time (*Materials and Methods*). The SPD provides a proxy measurement of the size of a prehistoric population with a level of precision and time resolution not currently attainable by any other technique. Using the SPD approach, we compare measurements of long-term population growth rates worldwide to investigate the impact of agriculture on the growth of prehistoric societies.

Results

We calculate the SPD for the states of Wyoming and Colorado from 7,900 radiocarbon measurements (*Materials and Methods*). Fig. 1 shows the SPD for the last 15,000 y on a log-linear scale. The population of Wyoming and Colorado 6,000–13,000 calibrated years before present (cal BP) is characterized by long-term exponential growth punctuated by short-term fluctuations on timescales of a few hundred to a thousand years. The leveling off and then decline of the SPD observed 3,000–6,000 cal BP

Significance

We statistically analyze the radiocarbon record and show that early farming societies in Europe grew at the same rate as contemporaneous foraging societies in North America. Thus, our results challenge the commonly held view that the advent of agriculture was linked to accelerated growth of the human population. The same rates of prehistoric population growth measured worldwide suggest that the global climate and/or biological factors intrinsic to the species and not factors related to the regional environment or subsistence practices regulated the growth of the human population for most of the last 12,000 y. This study demonstrates that statistical analysis of the radiocarbon record is a robust quantitative approach for studying prehistoric human demography.

Author contributions: H.J.Z., E.R., and R.L.K. designed research; H.J.Z., E.R., and R.L.K. performed research; H.J.Z. and E.R. contributed new reagents/analytic tools; H.J.Z., E.R., and R.L.K. analyzed data; and H.J.Z., E.R., and R.L.K. wrote the paper.

The authors declare no conflict of interest.

This article is a PNAS Direct Submission. S.J.S. is a guest editor invited by the Editorial Board.

[1]To whom correspondence may be addressed. Email: zahid@cfa.harvard.edu or erick.robinson@uwyo.edu.

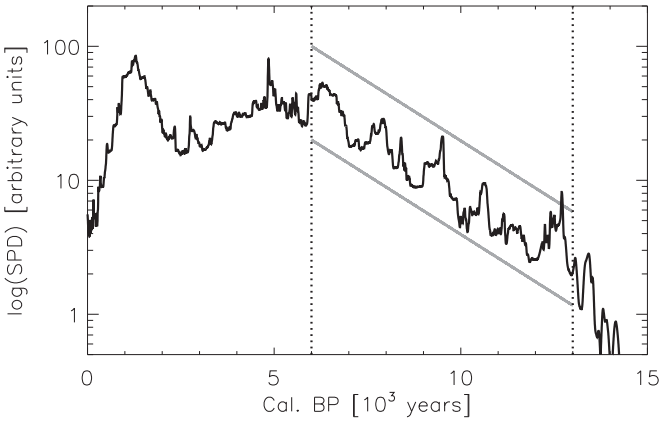

Fig. 1. The SPD for Wyoming and Colorado for the last 15,000 y plotted on a log-linear scale. The SPD is corrected for taphonomic loss (*Materials and Methods*). On this scale, the SPD 6,000–13,000 calibrated years before present (cal BP) appears to increase linearly. This scaling is a signature of exponential growth. The dotted lines delineate the time interval (6,000–13,000 cal BP) where the population is clearly undergoing long-term exponential growth. The solid gray lines are meant as a guide.

could be due to a declining growth rate of the population or migration out of the region.

We quantify the growth rate of the Wyoming and Colorado population 6,000–13,000 y ago by fitting an exponential model. Fig. 2*A* shows the best-fit model plotted over the SPD (*Materials and Methods*). For the population of Wyoming and Colorado 6,000–13,000 cal BP, we measure a long-term annual growth rate of $0.041 \pm 0.003\%$. Our measurement is consistent with a previous estimate of the North American population long-term annual growth rate of $0.05 \pm 0.03\%$ (26). The measurement of ref. 26 is based on radiocarbon data that are distributed throughout North America. The SPD derived by ref. 26 does not show a leveling off or decline in the population 3,000–6,000 cal BP. Thus, the leveling off and decline in the Wyoming and Colorado SPD are not part of a broader continental trend.

Fig. 2*B* shows the relative deviation of the data from the model. From these deviations, we estimate that ∼50% of the time the population of Wyoming and Colorado deviates from mean exponential growth by a factor of 1.25 or less and ∼90% of the time it deviates by a factor of 1.5 or less. The relative deviations appear to be symmetrically distributed and the magnitude of the fluctuations are time independent. Although some of the deviations are likely artificial spikes induced by the calibration procedure or statistical fluctuations due to data sampling, many deviations are real variations in the radiocarbon record (*Materials and Methods*) and thus interpreted as population fluctuations (28). These short-term fluctuations correspond to annual rates of growth/decline (averaged over 100 y) that are substantially greater (a factor of >10) than the long-term annual growth rate of 0.04%.

Fig. 3 shows measurements of the annual growth rate calculated from SPDs for North America (26), Australia (27), and Europe (28). The SPD comparison is restricted to studies that report measurements of the long-term growth rate. This restriction is necessary because growth rates measured on timescales less than a few thousand years are subject to short-term population fluctuations that may obfuscate long-term growth trends (e.g., see Fig. 2*A*). Fig. 3 also shows a measurement of the growth rate calculated from estimates of the global population that do not rely on the temporal frequency of radiocarbon data (32) (*Materials and Methods*). The growth rate calculated from these data are significant because the methodology used to estimate the population size is completely independent from our analysis and therefore provides an important cross-check on the systematic uncertainties of the SPD approach. Many studies have indicated that SPDs are valid demographic proxies (25–30, 33). Fig. 3 demonstrates that the SPD is a robust, unbiased proxy of relative population size that can be used to precisely and accurately measure the long-term rate of population growth.

Discussion

Measurements in Fig. 3 show remarkable agreement. Population growth across several continents and over long stretches of time appears to be consistent with a small annual rate of 0.04%. The data suggest that 0.04% is a long-term equilibrium annual rate of growth for human populations worldwide during much of the Holocene. This growth rate corresponds to a doubling of the population every ∼1,700 y.

Measurements in Fig. 3 allow us to assess the impact of agriculture on prehistoric population growth. During the period examined here, European societies were farming or transitioning to agriculture (28), whereas the inhabitants of Wyoming and Colorado were foraging for subsistence (34, 35). Despite these differences, the growth rates measured from SPDs of these two populations are consistent throughout much of the Holocene. Moreover, the short-term growth rate measured in 200-y bins for all of North America (26) shows no strong, secular deviations from the long-term annual growth rate of $0.05 \pm 0.03\%$ throughout 800–13,000 cal BP (figure 5 in ref. 26); this period includes the transition to agriculture in North America (36). Thus, the introduction of agriculture cannot be directly linked to an increase in the long-term annual rate of population growth. This conclusion is consistent with recent genetic analysis showing that human population expansion worldwide predated the introduction of agriculture (23, 24).

Within the uncertainties, the same rate of growth is measured for prehistoric human populations across a broad range of geographies and climates, environments that naturally have different carrying capacities. This similarity in growth rates suggests that prehistoric humans effectively adapted to their surroundings

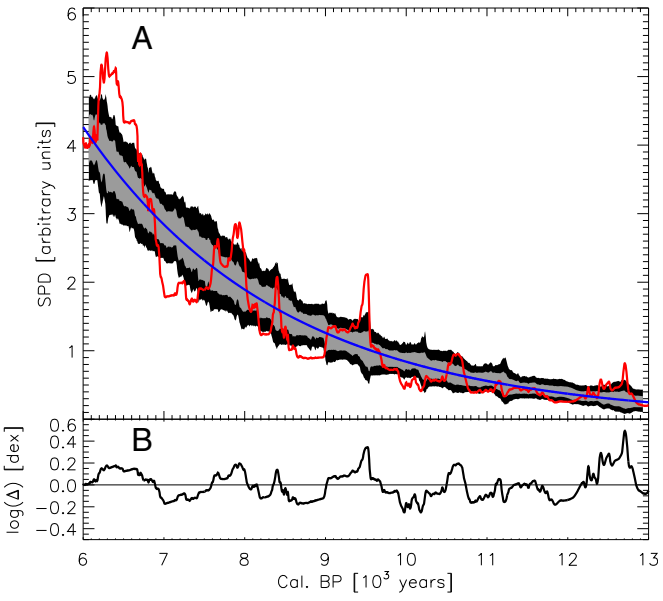

Fig. 2. (*A*) The SPD and best-fit exponential model are plotted in red and blue, respectively. The gray and black areas denote the 68% and 95% confidence intervals of the exponential model fit determined from bootstrapping (*Materials and Methods*). (*B*) The deviation of the data relative to the model (Δ = SPD/model) plotted on a logarithmic scale. Factors of 1.25 and 1.5 correspond to 0.10 and 0.18 dex, respectively.

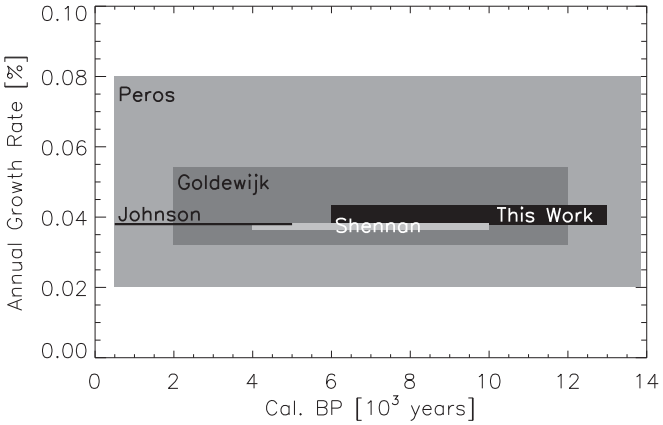

Fig. 3. The growth rate we measure ("This Work") and those found in the literature. Peros (26), Johnson (27), and Shennan (28) are measured from a SPD. Goldewijk (32) is calculated from population estimates found in the literature, which are not derived from the radiocarbon record. Goldewijk et al. (32) also examine population growth on each continent independently. They report continental growth rates of 0.03–0.05% for 2,000–12,000 cal BP (table 3 of ref. 32). The width of each box represents the 1σ error, and each box extends over the period in which the growth rate was measured. Johnson et al. did not provide an estimate of the error, and therefore their measurement is plotted as a line.

such that region-specific environmental pressure was not the primary mechanism regulating long-term population growth. Although the exact mechanisms remain uncertain, the consistency of the data indicates that these mechanisms must be something common to the species such as the global climate and/or endogenous biological factors. In contrast, the few hundred- to thousand-year short-term fluctuations observed in the SPDs could be caused by factors external to the population such as abrupt changes in the local climate (29, 37) or internal causes such as subsistence practices (28).

Fertility purportedly increased by two births per woman during the transition from foraging to farming (18). To maintain the constant long-term growth observed in all of the SPDs, any increase in fertility associated with the transition to agriculture must be short-lived or fertility and mortality must track each other closely in time. A short-term increase in only fertility or a temporal lag between long-term increases in fertility and mortality would result in a transient increase in the growth rate. Thus, demographic shifts resulting from the introduction of agriculture could manifest as short-term fluctuations in the SPD (28).

We estimate the total number of births per woman required to maintain a 0.04% annual growth rate using the Euler–Lotka equation (ref. 38 and references therein). A commonly used approximation of this equation is given by $r \sim \ln(R_0)/T_c$ (39), where r is the rate of growth, R_0 is the net reproduction rate, and T_c is the cohort generation time. We use the general integral form of the equation as follows:

$$\int_0^\infty e^{-ra}\, l(a)b(a)da = 1. \qquad [1]$$

This equation applies to all of the females of a population, where r is the population rate of growth, a is age in years, $l(a)$ is the survivorship curve, and $b(a)$ is the maternity curve. The survivorship curve parameterizes mortality, and the maternity curve parameterizes fertility. We adopt the average survivorship model curve for modern hunter-gathering societies with parameters given in ref. 40 (table 2). We parameterize the maternity curve by a Brass polynomial (41), which is shown to empirically fit fecundity distribution of mammalian populations (42). The curve is as follows:

$$b(a) = c(a-d)(d+w-a)^2, \qquad [2]$$

where we set $b(a) = 0$ for $a < d$ and $a > d + w$. Thus, d and $d + w$ are the youngest and oldest age a woman can give birth, respectively, and the integral given in Eq. **1** is zero when $b(a) = 0$. For this calculation, we set $d = 15$ and $w = 25$. The normalization parameter c is proportional to the number of female births per woman. We double the female number of births to get the total number of births we report. Based on the average survivorship of modern hunter-gatherers (40), 4.11 births per woman are required to maintain an annual growth rate of 0.04%.

Maintaining a small rate of growth for thousands of years requires fine-tuning of the parameters for maternity and survivorship in Eq. **1**. We calculate that a change of 0.04 in the number of births per woman (a 1% increase, i.e., going from 4.11 to 4.15), doubles the annual growth rate from 0.04% to 0.08% (a 100% increase). The growth rate is similarly hypersensitive to changes in the survivorship curve. A 1% increase in the probability that a woman lives to mean age of reproduction nearly doubles the annual rate of population growth. The hypersensitivity of the growth rate on survivorship and maternity is due to the fact that a growth rate of 0.04% (fractional rate of 0.0004) is $\ll 1$. The fine-tuning of survivorship and maternity required to maintain small, constant long-term growth throughout much of the Holocene requires that some mechanism or mechanisms force the difference between fertility and mortality toward equilibrium. If fertility increased substantially with the introduction of agriculture as some of evidence suggests (18), the hypersensitivity of the growth rate on maternity and survivorship underscores the necessity for fertility and mortality to track each other very closely.

We adopt the average survivorship curve of several modern hunter-gather societies to calculate the 4.11 births per woman required to maintain an annual growth rate of 0.04%. This average survivorship curve may not reflect the true survivorship of prehistoric societies, which is unknown. Thus, the number of births per woman we calculate is subject to large uncertainties. However, a key point of our demographic analysis is to show the hypersensitivity of the growth rate on maternity and survivorship. This hypersensitivity is independent of the particular parameterization of maternity and survivorship we adopt; it is solely a consequence of the very small rate of growth we measure.

The human population worldwide appears to have grown at a constant annual rate of 0.04% for most of the Holocene. With a world population of ~ 1 billion at AD 1800 (2), a 0.04% rate of growth retrodicts a global human population of a few individuals around 50,000 y ago. Although the population of anatomically modern humans was greater than few individuals at this time, archaeological and genetic studies agree it was very small and restricted to the African continent some time before 50,000 y ago (4, 5, 23, 43). The world population at AD 1800 is consistent with a small effective African population >50,000 y ago experiencing a long-term annual growth rate of 0.04%, and which most likely suffered decline during the severe climatic interval of the Glacial Maximum (44).

Conclusion

Statistical analysis of the radiocarbon record challenges the paradigm that the introduction of agriculture accelerated prehistoric population growth. The SPD analysis we present provides high time resolution measurements showing that population growth was sustained at near-equilibrium levels for thousands of years, irrespective of the local environment or subsistence strategy. However, the mechanisms for maintaining a

constant long-term growth rate modulated by short-term fluctuations during the period of human development we investigate here are uncertain. Our results suggest that statistical analyses of large ensembles of radiocarbon dates are robust demographic proxies of prehistoric human populations worldwide. This quantitative approach is valuable for further investigation of the mechanisms regulating human population growth.

Materials and Methods

We develop a suite of software to calibrate individual radiocarbon dates and produce the SPD of calibrated dates. Each date is calibrated using a Bayesian analysis (45) and the IntCal13 radiocarbon age calibration curve (46). The error in each ^{14}C measurement is translated into a probability distribution of calibrated dates. The parent radiocarbon data sample is composed of 7,986 dates. We remove 86 dates with ^{14}C measurement errors >300 y. The mode of the parent sample error distribution is 40 y. The 86 measurements we remove have errors that are outliers from the error distribution of the parent sample. We consider dates with such large errors potentially spurious measurements. We remove a very small fraction of our data due to large measurement errors; our conclusions are not effected by the exclusion of these dates. We sum the probability distribution of the remaining 7,900 individual dates to produce the SPD. Each date is equally weighted in the sum.

We correct the SPD for taphonomic loss using Eq. **1** in ref. 31:

$$N(t) = 5.726442 \times 10^6 (t + 2{,}176.4)^{-1.3925309}. \quad [3]$$

Here, $N(t)$ is expected to be constant and declines as a function of time t, given in units of calibrated years before present, due to taphonomic loss. Thus, we correct the SPD at each calibrated year by dividing by $N(t)$. As we show below, our results are not sensitive to this correction.

The combined uncertainties in the calibration curve, ^{14}C measurements, and data sampling rate produce uncertainties in the SPD. We simulate data to assess whether the short-term fluctuations observed in the SPD are significant. Fig. 2*A* shows the exponential model we derive from the data along with 68% and 95% confidence intervals, which are shown in gray and black, respectively. To derive these confidence intervals, we assume that the exponential model we fit to the data is the true underlying population distribution as a function of calibrated years before present. We randomly sample dates from the exponential model distribution, appropriately accounting for the number of measurements in our sample. We reverse calibrate our randomly sampled dates to get a simulated ^{14}C measurement. We assign a simulated error to each simulated ^{14}C measurement by randomly sampling the error distribution of the^{14}C measurements. We calibrate these simulated ^{14}C measurements and errors to produce a simulated SPD. We repeat this process to produce 1,000 simulated SPDs. The gray and black curves correspond to the 68% and 95% distribution of the simulated SPDs, respectively. The measured SPD deviates significantly from the simulated SPD. The null hypothesis that the measured SPD is derived from a purely exponential parent distribution is rejected. Thus, we conclude that the population of Wyoming and Colorado from 6,000–13,000 cal BP is characterized by long-term exponential growth that is punctuated by real short-term fluctuations.

In Fig. 2*A*, there are clear periods of time where the SPD (red curve) is skewed relative to the distribution of simulated SPDs (e.g., the spikes around 9,500 or 12,700 cal BP). The 68% and 95% confidence intervals indicate that large short-term spikes in the SPD coincide with regions where there is high variance in the simulated SPDs. These regions are susceptible to large systematic uncertainties induced by rapid changes in the calibration curve (47). The simulation analysis reveals that several large, few-hundred-year spikes are likely to be caused by the calibration curve and therefore not real spikes in the radiocarbon record. Conversely, this analysis also shows that there are many fluctuations in the data that we can confidently attribute to the radiocarbon record.

To measure the rate of growth for 6,000–13,000 cal BP, we fit a linear model to the logarithm of the SPD as a function of time. The slope of the fit is the exponential rate of growth, which we report as an annual percentage. The error is determined from bootstrapping the individual radiocarbon measurements. Bootstrapping accounts for the error in each data point and the sampling of the data. We also fit a generalized linear model (GLM) following the methodology of ref. 28. The GLM fit is consistent with our bootstrapping approach. Taphonomic correction can be large in an absolute sense. However, the rate of growth is a relative measure and therefore not very sensitive to the taphonomic correction in the time range we examine. If we do not correct the SPD for taphonomic loss, we measure an annual growth rate of 0.053 ± 0.003% for 6,000–13,000 cal BP.

We compare measurements of the rate of growth based on SPDs with independent measurements given in Goldewijk et al. (32). These authors provide estimates of the global human population and estimates of the population of each continent as a function of time. We fit the global data but note that the global and continental data yield consistent results [table 3 of Goldewijk et al. (32)]. The global data are taken from the supplementary table they provide. The data have a time resolution of 1,000 y. As before, we fit the logarithm of the population as a function of time with a linear model to measure the annual rate of growth. The authors quote an error of 100% for their population estimates for 2,000–12,000 cal BP. We propagate this error to the fit parameters. From population estimates given by Goldewijk et al., we calculate a global annual population growth rate of 0.043 ± 0.011% for 2,000–12,000 cal BP.

ACKNOWLEDGMENTS. We thank the anonymous reviewers for comments that significantly improved the manuscript. We thank Ben Johnson and Anna Barnacka for assistance in the statistical analysis, and Margaret Geller, Marc Vander Linden, Megan Taddonio, Hugh Hudson, and Anna Barnacka for careful reading of the manuscript. Mike Berry compiled the CO data. Nathaniel Kitchel and Justin McKeel curated data supplied by the Wyoming State Historic Preservation Office. H.J.Z. gratefully acknowledges the generous support of the Clay Postdoctoral Fellowship and encouragement from Margaret Geller. E.R. and R.L.K. are supported by NSF-1418858 (principal investigator, R.L.K.).

1. United Nations Department of Economic and Social Affairs (2013) *World Population Prospects: The 2012 Revision* (United Nations, New York).
2. Livi-Bacci M (2012) *A Concise History of World Population* (Wiley, Chichester, UK).
3. McDougall I, Brown FH, Fleagle JG (2005) Stratigraphic placement and age of modern humans from Kibish, Ethiopia. *Nature* 433(7027):733–736.
4. Behar DM, et al.; Genographic Consortium (2008) The dawn of human matrilineal diversity. *Am J Hum Genet* 82(5):1130–1140.
5. Mellars P (2006) Why did modern human populations disperse from Africa ca. 60,000 years ago? A new model. *Proc Natl Acad Sci USA* 103(25):9381–9386.
6. Bowler JM, et al. (2003) New ages for human occupation and climatic change at Lake Mungo, Australia. *Nature* 421(6925):837–840.
7. Higham T, et al. (2011) The earliest evidence for anatomically modern humans in northwestern Europe. *Nature* 479(7374):521–524.
8. Goebel T, Waters MR, O'Rourke DH (2008) The late Pleistocene dispersal of modern humans in the Americas. *Science* 319(5869):1497–1502.
9. Taylor KC, et al. (1993) The "flickering switch" of late Pleistocene climate change. *Nature* 361(6411):432–436.
10. Marcott SA, Shakun JD, Clark PU, Mix AC (2013) A reconstruction of regional and global temperature for the past 11,300 years. *Science* 339(6124):1198–1201.
11. Richerson PJ, Boyd R, Bettinger RL (2001) Was agriculture impossible during the Pleistocene but mandatory during the Holocene? A climate change hypothesis. *Am Antiq* 66(3):387–411.
12. Bocquet-Appel JP, Bar-Yosef O (2008) *The Neolithic Demographic Transition and Its Consequences* (Springer Science and Business Media, New York).
13. Cohen MN (1989) *Health and the Rise of Civilization* (Yale Univ Press, New Haven, CT).
14. Cohen MN (2009) Rethinking the origins of agriculture. Introduction. *Curr Anthropol* 50(5):591–595.
15. Bowles S (2011) Cultivation of cereals by the first farmers was not more productive than foraging. *Proc Natl Acad Sci USA* 108(12):4760–4765.
16. Bocquet-Appel JP (2002) Paleoanthropological traces of a Neolithic Demographic Transition. *Curr Anthropol* 43(4):637–650.
17. Eshed V, Gopher A, Gage TB, Hershkovitz I (2004) Has the transition to agriculture reshaped the demographic structure of prehistoric populations? New evidence from the Levant. *Am J Phys Anthropol* 124(4):315–329.
18. Bocquet-Appel JP (2011) When the world's population took off: The springboard of the Neolithic Demographic Transition. *Science* 333(6042):560–561.
19. Hawks J, Wang ET, Cochran GM, Harpending HC, Moyzis RK (2007) Recent acceleration of human adaptive evolution. *Proc Natl Acad Sci USA* 104(52):20753–20758.
20. Laval G, Patin E, Barreiro LB, Quintana-Murci L (2010) Formulating a historical and demographic model of recent human evolution based on resequencing data from noncoding regions. *PLoS One* 5(4):e10284.
21. Gignoux CR, Henn BM, Mountain JL (2011) Rapid, global demographic expansions after the origins of agriculture. *Proc Natl Acad Sci USA* 108(15):6044–6049.
22. Kelley JL (2012) Systematic underestimation of the age of selected alleles. *Front Genet* 3:165.
23. Zheng HX, Yan S, Qin ZD, Jin L (2012) MtDNA analysis of global populations support that major population expansions began before Neolithic Time. *Sci Rep* 2:745.
24. Aimé C, et al. (2013) Human genetic data reveal contrasting demographic patterns between sedentary and nomadic populations that predate the emergence of farming. *Mol Biol Evol* 30(12):2629–2644.

25. Riede F (2009) Climate and demography in early prehistory: Using calibrated ^{14}C dates as population proxies. *Hum Biol* 81(2-3):309–337.
26. Peros MC, Munoz SE, Gajewski K, Viau AE (2010) Prehistoric demography of North America inferred from radiocarbon data. *J Archaeol Sci* 37(3):656–664.
27. Johnson CN, Brook BW (2011) Reconstructing the dynamics of ancient human populations from radiocarbon dates: 10 000 years of population growth in Australia. *Proc Biol Sci* 278(1725):3748–3754.
28. Shennan S, et al. (2013) Regional population collapse followed initial agriculture booms in mid-Holocene Europe. *Nat Commun* 4:2486.
29. Kelly RL, Surovell TA, Shuman BN, Smith GM (2013) A continuous climatic impact on Holocene human population in the Rocky Mountains. *Proc Natl Acad Sci USA* 110(2):443–447.
30. Tallavaara M, Luoto M, Korhonen N, Järvinen H, Seppä H (2015) Human population dynamics in Europe over the Last Glacial Maximum. *Proc Natl Acad Sci USA* 112(27): 8232–8237.
31. Surovell TA, Finley JB, Smith GM, Brantingham PJ, Kelly R (2009) Correcting temporal frequency distributions for taphonomic bias. *J Archaeol Sci* 36(8):1715–1724.
32. Goldewijk KK, Beusen A, Janssen P (2010) Long-term dynamic modeling of global population and built-up area in a spatially explicit way: Hyde 3.1. *The Holocene* 20(4): 565–573.
33. Downey SS, Bocaege E, Kerig T, Edinborough K, Shennan S (2014) The Neolithic Demographic Transition in Europe: Correlation with juvenility index supports interpretation of the summed calibrated radiocarbon date probability distribution (SCDPD) as a valid demographic proxy. *PLoS One* 9(8):e105730.
34. Kelly RL, Todd LC (1988) Coming into the country: Early Paleoindian hunting and mobility. *Am Antiq* 53(2):231–244.
35. Frison GC (1998) Paleoindian large mammal hunters on the plains of North America. *Proc Natl Acad Sci USA* 95(24):14576–14583.
36. Smith BD (1995) *The Emergence of Agriculture* (Scientific American Library, New York).
37. Robinson E, Van Strydonck M, Gelorini V, Crombé P (2013) Radiocarbon chronology and the correlation of hunter gatherer sociocultural change with abrupt palaeoclimate change: The Middle Mesolithic in the Rhine-Meuse-Scheldt area of northwest Europe. *J Archaeol Sci* 40(1):755–763.
38. Smith DP, Keyfitz N, Wachter KW, Le Bras H (2013) *Mathematical Demography: Selected Papers* (Springer Science and Business Media, New York).
39. McCann JC (1973) A more accurate short method of approximating Lotka's *r*. *Demography* 10(4):567–570.
40. Gurven M, Kaplan H (2007) Longevity among hunter-gatherers: A cross-cultural examination. *Popul Dev Rev* 33(2):321–365.
41. Brass W, et al. (1975) *Methods for Estimating Fertility and Mortality from Limited and Defective Data* (University of North Carolina, Chapel Hill, NC).
42. Gage TB (2001) Age-specific fecundity of mammalian populations: A test of three mathematical models. *Zoo Biol* 20(6):487–499.
43. Mellars P, Gori KC, Carr M, Soares PA, Richards MB (2013) Genetic and archaeological perspectives on the initial modern human colonization of southern Asia. *Proc Natl Acad Sci USA* 110(26):10699–10704.
44. Bocquet-Appel JP, Demars PY, Noiret L, Dobrowsky D (2005) Estimates of Upper Palaeolithic meta-population size in Europe from archaeological data. *J Archaeol Sci* 32(11):1656–1668.
45. Ramsey CB (2009) Bayesian analysis of radiocarbon dates. *Radiocarbon* 51(1):337–360.
46. Reimer PJ, et al. (2013) Intcal13 and marine13 radiocarbon age calibration curves 0–50,000 years cal bp. *Radiocarbon* 55(4):1869–1887.
47. Brown WA (2015) Through a filter, darkly: Population size estimation, systematic error, and random error in radiocarbon-supported demographic temporal frequency analysis. *J Archaeol Sci* 53:133–147.